RECOVERY OF VALUABLE METALS FROM FLY ASH VIA HYDROMETALLURGY METHOD FOR LI-ION BATTERY ANODE MATERIAL

Cornelius Satria Yudha[1,2,*], Enni Apriliyani[1], Tika Paramitha[1,3], Windhu Griyasti Suci[1,2], and Himmah Sekar Eka Ayu Gustiana[1,2]

[1] *Centre of Excellence for Electrical Energy Storage Technology, Universitas Sebelas Maret, Surakarta, Indonesia*
Jl. Ir. Sutami 36A, Jebres, Kentingan, Surakarta, Central Java, Indonesia
[2] *Chemical Engineering Department, Vocational School, Universitas Sebelas Maret, Surakarta, Central Java, Indonesia*
Jl. Ir. Sutami 36A, Jebres, Kentingan, Surakarta, Central Java, Indonesia
[3] *Chemical Engineering Department, Engineering Faculty, Universitas Sebelas Maret, Surakarta, Indonesia*
Jl. Ir. Sutami 36A, Jebres, Kentingan, Surakarta, Central Java, Indonesia

*Correspondence, tel/fax : 0271-646994, email: coorneliussyudha@staff.uns.ac.id

ABSTRACT

Coal-derived fly ash, or CFA, is a harmful waste for humans. CFA waste handling by its processing and utilization has become the most promising approach, which not only decreases the waste's hazard level but also improves its economic potential. This research aims to recover metals from CFA and utilize them as anode material for Li-ion batteries. Iron, magnesium, aluminum, and calcium are retrieved from the CFA via a two-step hydrometallurgical method, i.e., acid leaching followed by alkaline precipitation. The leaching process utilizes various acids, such as acetic acid (CH_3COOH), hydrochloric acid (HCl) and sulfuric acid (H_2SO_4). Metal precipitation is carried out using sodium hydroxide solution (NaOH). Morphological and quantitative metal composition analysis are investigated using a scanning electron microscope and energy dispersive spectroscopy (SEM-EDX). The physical and chemical properties of the as-prepared samples are characterized using Fourier-transformed Infra-red spectroscopy (FTIR) and Thermal Gravimetry-Differential Thermal Analysis (TG/DTA). Based on the analysis, iron, magnesium and calcium are successfully recovered in a mixed hydroxide precipitate. The type of acid affects the final morphology and composition of the product. Therefore, our approach can be considered effective in CFA waste processing and producing high-quality product.

Keywords: coal-fly ash, hydrometallurgy, metal, precipitation, waste.

INTRODUCTION

Indonesia, as a country with a high population, has high domestic energy demand. Therefore, fuel and electricity supplies are always the nation's primary concern. Based on the statistical data provided by BPS (Badan Pusat Statistik or

Statistics Indonesia), Indonesian annual capital energy demand is 1.1 MWh. Moreover, based on data from the State Electricity Company or PLN, this energy demand is expected to increase up to 20% by 2030 with a total of 390 TWh annual energy demand. On the other hand, the energy share is still dominated by fossil fuels, particularly coal [1].

Coal power plant releases wastes, including emission and fly ash. Coal fly ash or CFA is categorized as hazardous waste due to its ability to contaminate water and soil with heavy metals and cause health issues for humans, i.e. lung, kidney, and gastrointestinal diseases or illness [2]. In every CFAs, trace heavy metals with a concentration of more than one ppm, such as Pb, Zn, Cu, Cd, Cr, and As, can be found. When discarded inappropriately, the metals will ultimately be exposed to the environment, especially water bodies [3].

Several efforts are extensively performed to handle the CFA waste. For instance, CFAs are used as an ingredient for construction material (Portland cement) and agricultural purposes [4,5]. It contains minerals and silica that can be purified into new materials with economic value. Several studies showed that CFA could be used as a catalyst, adsorbent, carbon capture material, and semi-conductor [6]. Mainly, these applications rely on the utilization of silica or silicon dioxide, which has the most significant proportion in fly ash [7]. The metals such as iron (Fe), aluminum (Al) and calcium are rarely utilized. The total concentration of the metal oxides is about 10-40%; in other words,

for every ton of CFAs, a potential 40 kg of metal oxide is potentially recovered. This significant amount of metals requires consideration, especially for its utilization [8].

Li-ion battery technology attracts industries' interest due to its ability as the power source of electric vehicles and power tools [9]. Inside the battery are active materials for the anode and cathode. The commercial battery has artificial graphite as the anode. It has a moderate specific capacity and is highly abundant. However, synthesizing graphite anode requires high energy [10]. Naturally mined graphite can replace artificial graphite; however, it has low purity, which can severely affect the cells' performance [11]. These confirmed that developing anode materials from cheap and abundant resources and moderate processing conditions are necessary. Not only can it significantly reduce the economic challenges, but it can also improve the materials' eco-friendliness. Thus, using CFAs for the anode material precursor is a strong candidate for such anode material.

The transitional metal-based anode is a novel anode material that can store Li ions using a conversion mechanism [12]. For instance, iron oxide derived from iron hydroxide anode material can deliver a discharge capacity of 950 mAh/g, almost three times higher than graphite [13]. Another study shows good utilization of iron hydroxide anode material with a high capacitance of ~1 kFarad/g [14]. A study by Quinzeni, *et. al.* reported the possibility of Ca-Al doped iron oxide material as anode material showing a reversible capacity of ~950 mAh/g. Thus, this

material can be easily prepared using various metal sources, especially CFAs, under mild conditions. Therefore, for the first time in this study, the metals in CFA are extracted using acid and precipitated using an alkaline solution or sodium hydroxide. Various studies suggest using ammonia as a precipitant; however, it is unsafe for the environment. To extract the metals, we use cheap acids such as hydrochloric acid (HA), sulfuric acid (SA), and acetic acid (AA). Besides their economic attractiveness, these acids are reactive towards metal oxide mixtures, sTable toward high temperatures, have excellent kinetics, high purity, and high availability [15–17]. The resulting precipitates are evaluated using FTIR spectroscopy and SEM-EDX analysis. The precipitates are also used as the anode material of Li-ion batteries to measure their storage capacity and performance.

METHODS
Tools and Materials

Coal combustion fly ash or CFA was obtained from Paiton Power Plant, Probolinggo, East Java, Indonesia. Glacial acetic acid 99.5% v/v (CH_3COOH), hydrochloric acid 37% v/v (HCl), and sulfuric acid 98% v/v were obtained from Merck, Germany. Sodium hydroxide (NaOH) 95% was obtained from PT Asahimas Chemical Indonesia. Besides the CFA, all of the materials were used without a further purification step.

An overhead stirrer and A 500 mL beaker glass were used as the leaching reactor. A controllable hot plate was used to control the temperature of the reaction. Filter papers, funnels and flasks were used during the filtration process. An atmospheric drying oven and crucibles were used during the drying process.

Sample Preparation

15 g of dried CFA were added in 150 ml of each acid (HA/SA/AA) with 4 M concentration. The acid leaching was conducted in a beaker glass with continuous stirring at 60 °C for 3 hours. Higher acid concentration is considered harmful, while lower concentration is deemed to have low reactivity, resulting in low metal recovery. Next, 200 mL of distilled water was added to the beaker, followed by another hour of stirring. The slurry was filtered, and the filtrate was reacted with 2 M of NaOH until a pH of 13 was reached. At elevated pH, a reddish precipitate was formed. The precipitate was filtered, washed until neutral using demineralized water and ethanol and labelled as P-HA, P-SA, and P-AA, respectively, towards the leaching agents.

Sample characterizations and electrochemical performance evaluation

The functional group of the samples were analyzed using Fourier-Transformed Infra-Red Spectroscopy (FTIR, IR-Spirit, Shimadzu, Japan). The morphology of the samples was investigated using a scanning electron microscope (SEM, JCM-7000, Jeol, Japan), and the elemental composition was studied using Energy Dispersive X-ray (EDX). The thermal behaviour of the sample was analyzed using Thermal Gravimetry and Differential Thermal Analysis (TG/DTA, Shumadzu DTG-60, Japan). The electrochemical performance was evaluated in a Li-ion battery, where the samples were

used as an anode material. The assembly process was performed according to our previous study [18]. Lithium nickel manganese cobalt oxide (NMC622) was used as the cathode material. The cathode and anode sheets were fabricated by mixing each powder with carboxymethyl cellulose (CMC), styrene butadiene rubber (SBR), and carbon black (CB) at a mass ratio active material CMC:SBR:CB = 90:3:2:5. Then it dispersed in demineralized water to obtain a slurry. Each slurry was then coated with 0.2 mm thickness. The mass loading of the cathode and anode is 18 mg/cm^2 and 35 mg/cm^2. The electrodes were separated using a polypropylene separator and rolled using a rolling machine to obtain a battery jelly roll. This roll was placed in a cylindrical case. After the cell was assembled, LiPF$_6$ electrolyte was added to the cell. The cell is ready to be tested using Neware Battery Analyzer (Neware, China). The voltage window was set to 2-4.3 V.

RESULTS AND DISCUSSION

Coal fly ash obtained from Paiton Power Plant was initially characterized to ensure its morphological feature and elemental composition. The SEM-EDX analysis result can be seen in Figure 1.
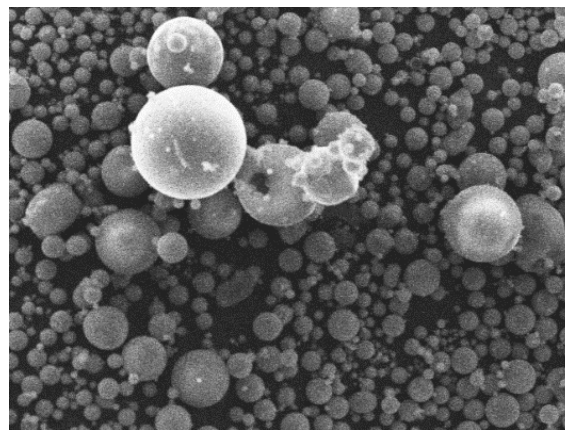
(a)
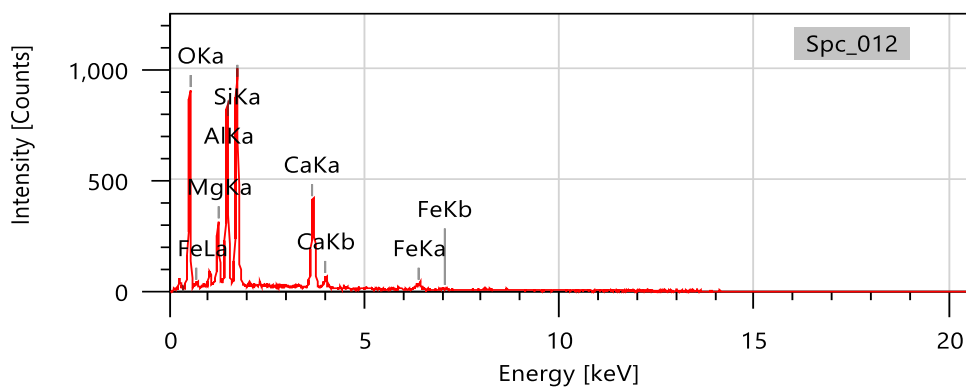
(b)

Figure 1. CFA analysis result by (a) SEM and (b) SEM-EDX

Figure 1 (a) shows the morphology of the Paiton Power Plant at 1000x magnification. The CFA has a homogenous spherical shape with micron-sized particles with narrow particle size distribution. This type of morphology is beneficial during the extractive leaching process due to the similar condition and leaching mechanism between one particle and another. Therefore, the leaching kinetic studies are attractive for future studies. The EDX analysis in Figure 1 (b) is quantitatively determined with the result shown in Table 1. Based on our findings, the CFA is classified as Type-F fly ash due to the dominant presence of silicon, aluminum, and iron rather than calcium. The presence of aluminum and iron is beneficial for anode material fabrication since iron and aluminium have good electrochemical properties such as conductivity, Li-ion storage, and redox ability which is essential [19–22].

Table 1. Elemental analysis of Coal Fly Ash from Paiton Power Plant

Element	Wt%	Mol%
C	4.68	8.55
O	42.12	57.72
Mg	2.61	1.79
Al	10.64	8.64
Si	16.21	12.69
Ca	8.42	4.62
Fe	15.32	5.99
Total	100	100

In this report, the CFA was leached using H_2SO_4 (SA), HCl (HA), and CH_3COOH (AA). The as-obtained leaching solution was reacted with NaOH to recover the valuable metals in the form of mixed hydroxide (P). The hydroxide precipitates were analyzed using FTIR spectroscopy and EDX to identify the functional groups present in the sample.

It is estimated that the samples are obtained from the following double replacement reactions:

$$M_xO_{y(s)} + H_aA_{b(aq)} \rightarrow M_aA_{y(aq)} + H_2O_{(l)} \quad (1)$$

Where: M= Al, Fe, Mg, Ca

A= SO_4, CH_3COO, Cl

The precipitation occurred caused by the low solubility of the product, which is $Al(OH)_3$, $Ca(OH)_2$, $Fe(OH)_3$. It is according to the following equation:

$$M_aA_{y(aq)} + NaOH_{(aq)} \rightarrow M(OH)_{y(s)} + Na_aA_{(aq)} \quad (2)$$
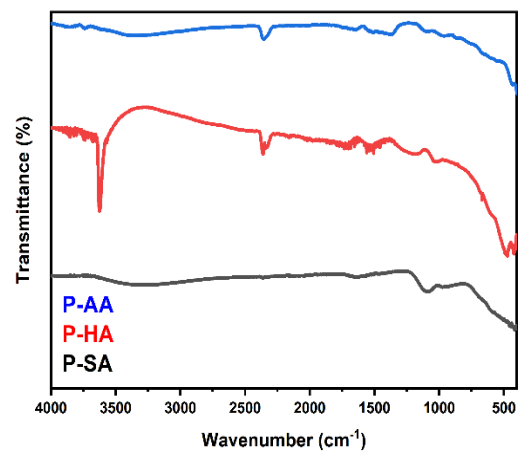
Figure 2. FTIR spectroscopy of precipitate samples obtained by various acids

The elemental composition of the precipitates from quantitative analysis using EDX is listed in Table 2.

Table 2. Elemental analysis of mixed hydroxides derived from fly ash

Element	P-SA (mol%)	P-HA (mol%)	P-AA (mol%)
Mg	10.98	6.33	12.4
Al	10.78	7.62	15
Ca	1.74	70.88	10.51
Fe	69.49	15.12	51.73
S	6.99	0	0
Cl	0	0.05	0
Na	0.02	0	0.02
C	0	0	10.34
Total	100	100	100

Figure 2 presents the FTIR spectra of the precipitates leached by various acids. Among three samples, the P-HA shows a hydroxyl functional group absorption peak at ~3600/cm, corresponding to the presence of $M(OH)_x$ or metal hydroxide [23]. Broad hydroxyl peaks in P-SA and P-AA indicate a small number of hydroxide species. The double absorption peaks at ~2300/cm confirm the presence of carbon dioxide molecules during the testing [24,25].

Based on Table 2, the acids significantly affect the composition of the precipitate. The selectivity of the acids towards the leaching of the element can cause this. For instance, sulfuric acid has low selectivity towards Ca due to the formation of a $CaSO_4$ (eq (3)) solid, which is insoluble in various acids [26]. Therefore, SA sample has the highest Fe and lowest Ca content compared to HA and AA.

$$CaO_{(s)} + H_2SO_4 \rightarrow_{(aq)} CaSO_{4(s)} + H_2O_{(l)}   (3)$$
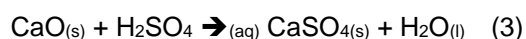
Samples were analyzed using TG/DTA analysis to ensure the presence of hydroxides. The TG/DTA curves of the samples can be seen in Figure 3.

(a)

(b)

(c)
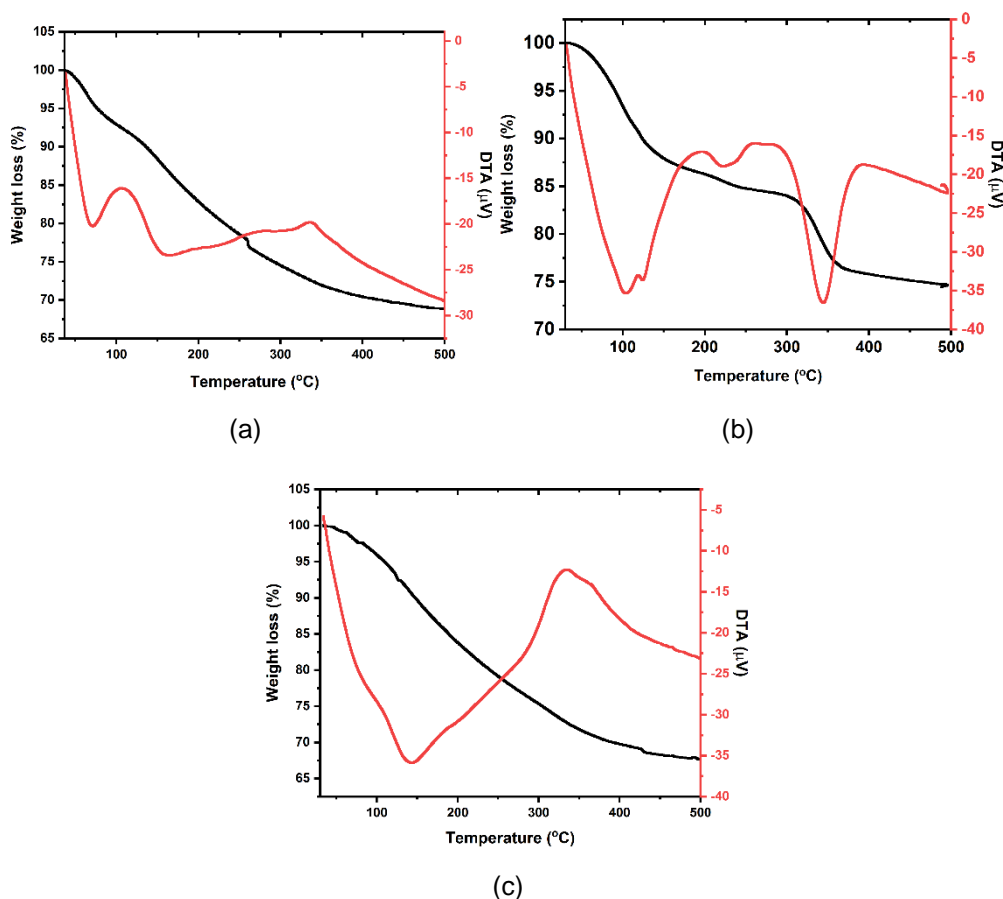
Figure 3. TG/DTA curve of (a) P-SA, (b) P-HA, and (c) P-AA

Based on the TG/DTA analysis, significant mass loss and an endothermic peak below 150 oC can be attributed to moisture in the samples. A continuous mass loss occurred, and the DTA peak at 330 indicates the dehydration or thermo-

decomposition of hydroxides. The sharpness of the peaks indicates the hydroxide content of the sample. The broad peak found in the P-SA sample proved that the sample has a low hydroxide level. It can be caused by the formation of oxide or oxy-hydroxide instead of hydroxide during the precipitation process (eq 4-6) due to the high level of Fe content. In primary conditions, iron can undergo different precipitate formation such as iron hydride ($Fe(OH)_3$). However, the presence of O_2 promotes the formation of oxyhydroxide FeOOH with similar iron valency of 3+. The iron oxidized iron (III) hydroxide can form into the intermediate FeOOH or further oxidized into iron (III) oxide hydrates. At elevated temperatures, dehydration occurred, which means that the sample lost its hydrate crystal; hence, sTable iron oxide was formed. The estimated reaction can be seen in the following equations [27–30]:

$$Fe^{3+} + NaOH \rightarrow Fe(OH)_{3(s)} \qquad (4)$$
$$2Fe(OH)_3 \rightarrow Fe_2O_3 \cdot 3H_2O \qquad (5)$$
$$Fe_2O_3 \cdot 3H_2O \rightarrow Fe_2O_3 + 3H_2O \qquad (6)$$
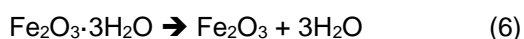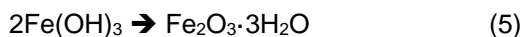
It can be noticed that sample P-HA with a high Ca level has a sharper dehydration peak, consistent with the FTIR result. Based on this evidence, the functional group of the precipitate is highly affected by the iron content. Higher iron content means higher oxide and lower hydroxide content in the sample, as stated in reactions 4-6. On the contrary, with low iron content, the metals such as Ca, Mg and Al tend to form hydroxides. The oxides formation of all elements can also be developed for future projects by additional heating or calcination/sintering process. With all oxide,

the determination of the samples' functional groups becomes easier to perform.

The morphology of all samples was investigated using SEM. The SEM images of the samples are displayed in Figure 4. Sample P-SA appears to have a quasi-spherical morphology with a particle size of 4-14 micrometres, and the particle's surface appears rough, with adherents around the particle. In addition, it has two types of particles, such as primary particles, which have a sub-micron size and similar shape, and secondary particles consist of agglomeration of primary particles [31]. P-SA sample is very distinctive toward P-HA and P-AA. The P-HA and P-AA samples have an irregular secondary shape with a semi-smooth surface. Based on the particle distribution, the P-SA sample has narrower particles than P-AA and P-HA, which have wide particle distribution confirmed by the extreme difference in particle sizes. The wide particle size range can cause inhomogeneous electrochemical reactions during the utilization of Li-ion batteries. The inhomogeneous reaction occurs due to a gradient of Li-ion concentration in electrolytes due to un-similar particle shapes and sizes [32,33]. A particle with small sizes tends to have a large surface area favourable toward Li-ion transfer. However, large area of particle can cause side reactions between electrolyte and the material and promote the solid electrolyte interphase or SEI, which consume a significant amount of lithium from the cathode [34]. The consumed Li cannot be recovered; hence a considerable capacity loss can be expected, especially during the initial formation phase or the first cycle.

Figure 5 displays the charge-discharge curve of three cells containing P-SA, P-HA, and P-AA as the anode material. $LiNi_{0.6}Mn_{0.2}Co_{0.2}O_2$ was used as the counter electrode. The theoretical discharge capacity of the cathode is 200 mAh/g. The anode was set as the weight basis during the calculation.

(a)

(b)

(c)
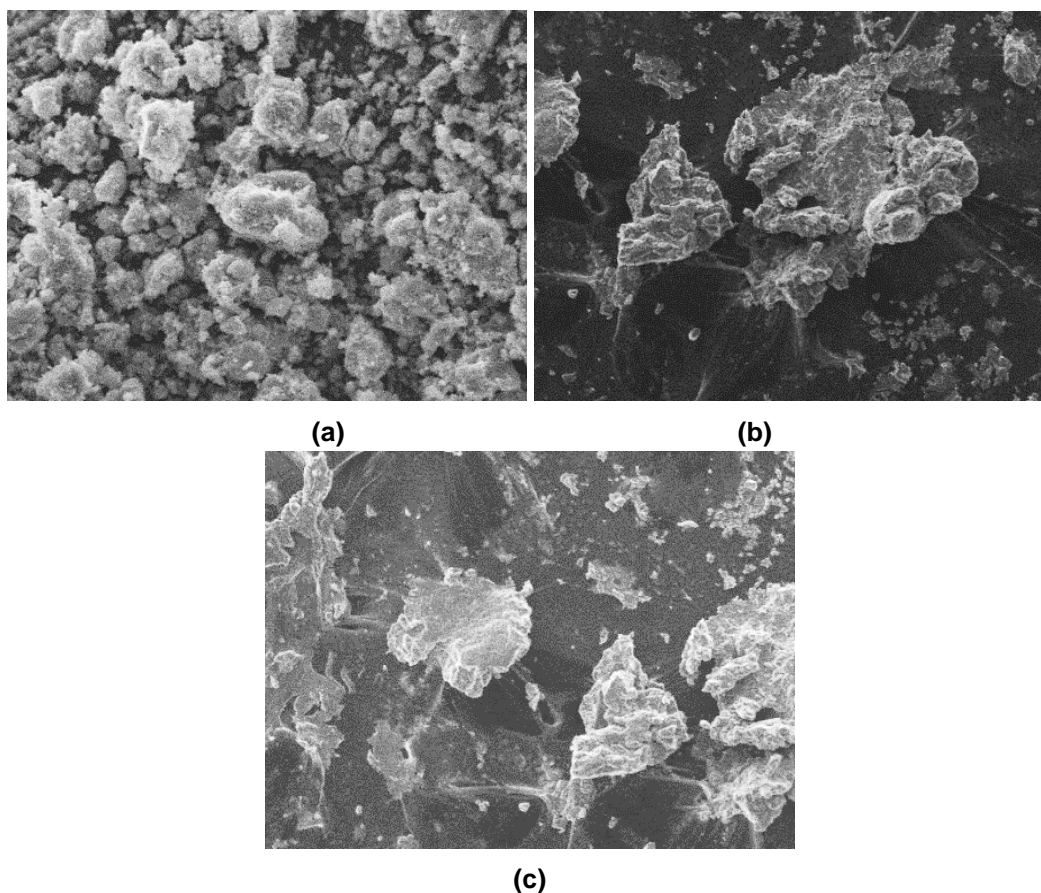
Figure 4. SEM Images of (a) P-SA, (b) P-HA, and (c) P-AA at 1000x magnification

Figure 5(a) shows that the tested samples have a similar charge-discharge curve. The charge curve can be seen rising from 0 voltage to 4.3 volts. The discharge curve can be seen declining as the specific capacity increases with the voltage cut-off at 2.0 V. The specific charge capacities of P-SA, P-HA, and P-AA are 707 mAh/g, 361 mAh/g and 767 mAh/g, respectively, while the discharge capacities are 511 mAh/g, 191 mAh/g, and 461 mAh/g, respectively. Hence, the initial coulombic efficiency (ICE) of P-SA, P-HA, and P-AA are 72.8%, 52.9%, and 60.1%, respectively. The result is in agreement with the SEM study. The highest specific capacity and ICE are achieved by P-SA, which can be attributed to the high iron content in the sample [15,18]. P-HA with high Ca content has the lowest specific capacity, and ICE explained that Ca has low electrochemical activity compared to the other elements in the sample. The cycle test at a similar current density also confirms the iron-rich anode material's stability (Figure 5(b)). The discharge capacity of P-SA, P-HA, and P-AA after 50 cycles are 80.3 mAh/g, 0 mAh/g and 24.3 mAh/g with calculated capacity retention of 15,6%, 0%, and 5.2%,

respectively. Therefore, sulfuric acid is beneficial for forming anode material from CFA with good electrochemical properties compared to the other acids, mainly due to a high amount of Fe in the sample. Selective leaching of Fe from CFA would be an exciting topic for future research [35]. However, many improvements are still required to improve the cycle-ability of the sample as anode materials. The upgrades can be performed by

improving the homogeneity of the particle morphology, purification from Ca and addition of a pre-lithiation process to enhance the ICE level. The morphology control can be achieved by several techniques, such as adding chelating agents and modifying co-precipitation parameters, such as controlled nucleation using microwave or ultrasonic technology [36,37].

(a)   (b)
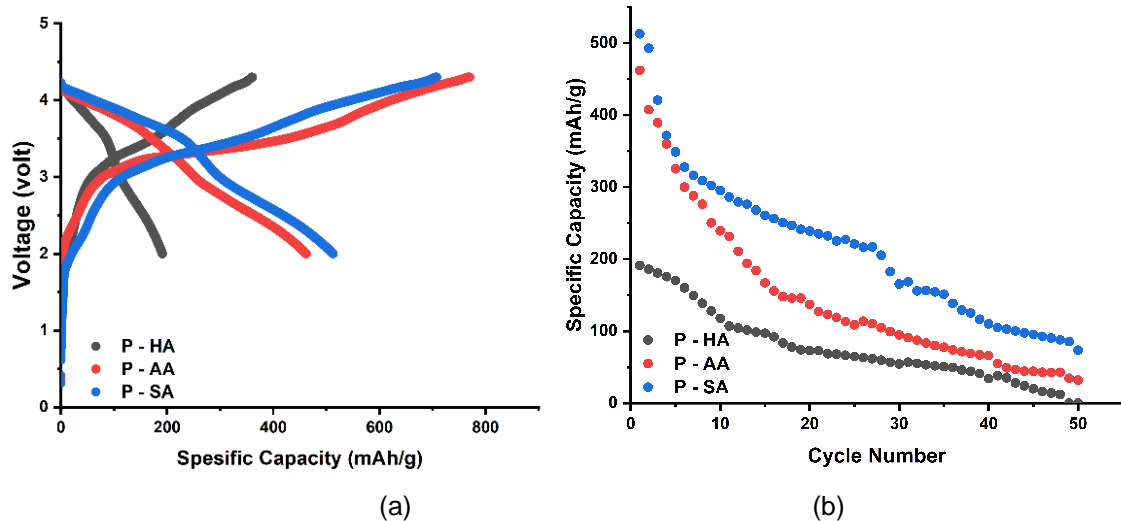
Figure 5. (a) Charge-discharge curve and (b) cycle-test of cells with P-SA, P-HA, and P-HA anode

CONCLUSION

Coal-fly ash is a promising precursor to anode materials for Li-ion batteries. The utilization of valuable metals from CFA as anode material is successfully conducted. Various acids were employed as the leaching agents, and NaOH was used as the precipitating agent to recover the metals. The deep characterization via FTIR, SEM, and TG-DTA confirmed that sulfuric acid is the most promising to be used as a leaching agent due to its selectivity toward electrochemically active material such as iron. The as-prepared anode material also has successfully applied in Li-ion battery cells. However, further research is urgently

needed, such as optimizing leaching parameters, additional post-treatments and structural analysis. The capacity drop observed in the study also proved that a modification of the as-prepared material should be developed. Despite it, the overall research still shows a promising result for the future generation of energy storage. The approach also can be applied as a method to process CFA waste in an environmentally friendly way.

ACKNOWLEDGEMENT

REFERENCES

[1]   J. Martínez-Lao, Montoya, F. G. Montoya, M.G. Montoya, F. Manzano-Agugliaro, "Electric Vehicles in Spain: An Overview of Charging Systems," *Renew. Sustain. Energy Rev.*,vol. 77, pp. 970–983, 2017, doi: 10.1016/j.rser.2016.11.239.

[2]   Y. Xing, F. Guo, M. Xu, X. Gui, H. Li, G. Li, Y. Xia, H. Han, "Separation of Unburned Carbon from Coal Fly Ash: A Review," *Powder Technol.,* vol. 353, pp. 372–384, 2019, doi: 10.1016/j.powtec.2019.05.037.

[3]   Verma, C.; Verma, R. Leaching Behaviour of Fly Ash: A Review. *Nat. Environ. Pollut. Technol.* vol. 18, pp. 403–412, 2019.

[4]   M. A. Kamal, "Recycling of Fly Ash as an Energy Efficient Building Material: A Sustainable Approach," *Key Eng. Mater,* vol. 692, pp. 54–65, 2016, doi:10.4028/www.scientific.net/KEM.692.54.

[5]   S. Ramanathan, S. C. B. Gopinath, M. K. M. Arshad, P. Poopalan, "Nanostructured Aluminosilicate from Fly Ash: Potential Approach in Waste Utilization for Industrial and Medical Applications," *J. Clean. Prod,* vol. 253, pp. 119923, 2020, doi: 10.1016/j.jclepro.2019.119923.

[6]   A. Dindi, D. V. Quang, L. F. Vega, E. Nashef, M. R. M. Abu-Zahra, "Applications of Fly Ash for CO_2 Capture, Utilization, and Storage," *J. CO2 Util.,* vol. 29, pp. 82–102, 2019, doi: 10.1016/j.jcou.2018.11.011.

[7]   A. Jumari, C. S. Yudha, H. Widiyandari, A. P. Lestari, "SiO2/C Composite as a High Capacity Anode Material of LiNi0.8Co0.15Al0.05O2 Battery Derived from Coal Combustion Fly Ash," *Appl. Sci.*, vol. 10, pp. 1–13, 2020, doi: 10.3390/app10238428.

[8]   M. G. Miricioiu and V. C. Niculescu, "Fly Ash, from Recycling to Potential Raw Material for Mesoporous Silica Synthesis," *Nanomaterials,* vol. 10. pp. 1–14, 2020, doi: 10.3390/nano10030474.

[9]   M. Li, J. Lu, Z. Chen, K. Amine, "30 Years of Lithium-Ion Batteries," *Adv. Mater*, vol. 30, no. 33, 2018, doi: 10.1002/adma.201800561.

[10]   C. S. Yudha, M. Rahmawati, A. Jumari, A. P. Hutama, A. Purwanto, "Synthesis of Zinc Oxide (ZnO) from Zinc Based-Fertilizer as Potential and Low-Cost Anode Material for Lithium Ion Batteries," *Proceedings of the ACM International Conference Proceeding Series; Association for Computing Machinery*, pp. 1–6, 2020, doi: 10.1145/3429789.3429860.

[11]   E. A. Olivetti, G. Ceder, G. G. Gaustad, X. Fu, "Lithium-Ion Battery Supply Chain Considerations: Analysis of Potential Bottlenecks in Critical Metals," *Joule*, vol. 1, no. 2, pp. 229–243, 2017, doi: 10.1016/j.joule.2017.08.019.

[12]   P. Long, Q. Xu, G. Peng, X. Yao, X. Xu, "NiS Nanorods as Cathode Materials for All-Solid-State Lithium Batteries with Excellent Rate Capability and Cycling Stability," *ChemElectroChem,* vol. 3, no. 5, pp. 764–769, 2016, doi: 10.1002/celc.201500570.

[13]   M. Du, C. Xu, J. Sun, L. Gao, "Synthesis of α-Fe2O3 Nanoparticles from Fe(OH)3 Sol and Their Composite with Reduced Graphene Oxide for Lithium Ion Batteries," *J. Mater. Chem. A.,* vol. 1, no. 24, pp. 7154–7158, 2013, doi: 10.1039/c3ta00183k.

[14] K. A. Owusu, L. Qu, J. Li, Z. Wang, K. Zhao, C. Yang, K. M. Hercule, C. Lin, C. Shi, Q. Wei, et al., "Low-Crystalline Iron Oxide Hydroxide Nanoparticle Anode for High-Performance Supercapacitors," *Nat. Commun.,* vol. 8, 2017,
doi: 10.1038/ncomms14264.

[15] S. U. Muzayanha, C. S. Yudha, L. M. Hasanah, A. Nur, A. Purwanto, "Effect of Heating on the Pretreatment Process for Recycling Li-Ion Battery Cathode," *JKPK (Jurnal Kim. dan Pendidik. Kim,* vol. 4. no. 2, 2019,
doi: 10.20961/jkpk.v4i2.29906.

16] X. Xiao, B. W. Hoogendoorn, Y. Ma, S. A. Sahadevan, J. M. Gardner, K. Forsberg, R. T. Olsson, "Ultrasound-Assisted Extraction of Metals from Lithium-Ion Batteries Using Natural Organic Acids," *Green Chem,* vol. 23, no. 21, pp. 8519–8532, 2021,
doi: 10.1039/d1gc02693c.

[17] S. U. Muzayanha, C. S. Yudha, A. Nur, H. Widiyandari, H. Haerudin, H. Nilasary, F. Fathoni, A. Purwanto, "A Fast Metals Recovery Method for the Synthesis of Lithium Nickel Cobalt Aluminum Oxide Material from Cathode Waste," *Metals (Basel),* vol. 9. no. 5, pp. 615, 2019,
doi: 10.3390/met9050615.

[18] C. S. Yudha, L. M. Hasanah, S. U. Muzayanha, H. Widiyandari, A. Purwanto, "Synthesis and Characterization of Material LiNi0.8Co0.15Al0.05O2 Using One-Step Co-Precipitation Method for Li-Ion Batteries," *JKPK (Jurnal Kim. dan Pendidik. Kim.,* vol. 4. no. 3, pp. 134, 2019,
doi: 10.20961/jkpk.v4i3.29850.

[19] P. Tanikella and J. Olek, "Updating Physical and Chemical Characteristics of Fly Ash for Use in Concrete," *JTRP Tech. Rep.,* 2017,

doi: 10.5703/1288284315213.

[20] I. Quinzeni, V. Berbenni, D. Capsoni, M. Bini, "Ca- and Al-Doped $ZnFe_2O_4$ Nanoparticles as Possible Anode Materials," *J. Solid State Electrochem,* vol. 22, pp. 2013-2024, 2018,
doi: 10.1007/s10008-018-3901-7.

[21] Y. Yuan, S. Liang, W. Liu, Q. Zhao, P. Peng, R. Ding, P. Gao, X. Sun, E. Liu, "Al-Doped Fe_2O_3 nanoparticles: Advanced Anode Materials for High Capacity Lithium Ion Batteries," *Dalt. Trans.,* vol. 50, no. 15, pp. 5115-5119, 2021,
doi: 10.1039/d0dt04423g.

[22] S. Wei, D. Di Lecce, D.; R. M. D'Agostini, J. Hassoun, "J. Synthesis of a High-Capacity α-Fe2O3@C Conversion Anode and a High-Voltage LiNi0.5Mn1.5O4Spinel Cathode and Their Combination in a Li-Ion Battery," *ACS Appl. Energy Mater.,* vol. 4, no. 8, pp. 8340-8349, 2021,
doi: 10.1021/acsaem.1c01585.

[23] C. S. Yudha, S. U. Muzayanha, H. Widiyandari, F. Iskandar, W. Sutopo, A. Purwanto, "Synthesis of LiNi0.85Co0.14Al0.01O2 Cathode Material and Its Performance in an NCA / Graphite Full-Battery," *Energies,* vol. 12, no. 10, pp. 1886, 2019,
doi: 10.3390/en12101886.

[24] F. Rolle and M. Sega, "Use of FTIR Spectroscopy for the Measurement of CO 2 Carbon STable Isotope Ratios," *Proceedings of the 19th International Congress of Metrology*, vol. 05002, pp. 1–6, 2019,
doi: 10.1051/metrology/201905002.

[25] K. Coenen, F. Gallucci, B. Mezari, E. Hensen, M. van Sint Annaland, "An In-Situ IR Study on the Adsorption of CO2 and H2O on Hydrotalcites," *J. CO2 Util.,* vol. 24, pp. 228-239, 2018,
doi: 10.1016/j.jcou.2018.01.008.

[26] D. Valeev, A. Mikhailova, A. Atmadzhidi, "Kinetics of Iron Extraction from Coal Fly Ash by Hydrochloric Acid Leaching. *Metals (Basel),* vol. 8, no. 7, pp. 1-9, 2018, doi: 10.3390/met8070533.

[27] A. L. Mackay, "β-Ferric Oxyhydroxide," *Mineral. Mag. J. Mineral. Soc.,* vol. 32, no. 250, pp. 545-557, 1960, doi:10.1180/minmag.1960.032.250.04.

[28] L. Gulina, V. Tolstoy, L. Kuklo, V. Mikhailovskii, V. Panchuk, V. Semenov, "Synthesis of $Fe(OH)_3$ Microtubes at the Gas–Solution Interface and Their Use for the Fabrication of Fe_2O_3 and Fe Microtubes," *Eur. J. Inorg. Chem.,* vol. 2018, no. 17, pp. 1842-1846, 2018, doi: 10.1002/ejic.201800182.

[29] S. K. Kwon, K. Kimijima, K. Kanie, A. Muramatsu, S. Suzuki, E. Matsubara, "Suppression of the Conversion Process of $Fe(OH)_3$ to β-FeOOH and α-Fe_2O_3 by Silicate Ions," *High Temp. Mater. Process.,* vol. 24, no. 5, pp. 275-287, 2005, doi: 10.1515/HTMP.2005.24.5.275.

[30] M. Mohapatra and S. Anand, "Synthesis and Applications of Nano-Structured Iron Oxides/Hydroxides – a Review," *Int. J. Eng. Sci. Technol.,* vol. 2, no. 8, pp. 127-146, 2011, doi: 10.4314/ijest.v2i8.63846.

[31] S. Takanashi and Y. Abe, "Improvement of the Electrochemical Performance of an NCA Positive-Electrode Material of Lithium Ion Battery by Forming an Al-Rich Surface Layer," *Ceram. Int.,* vol. 43, no. 12, pp. 9246-9252, 2017, doi: 10.1016/j.ceramint.2017.04.080.

[32] E. R. Logan, H. Hebecker, X. Ma, J. Quinn, Y. HyeJeong, S. Kumakura, J. Paulsen, J. R. Dahn, "A Comparison of the Performance of Different Morphologies of LiNi 0.8 Mn 0.1 Co 0.1 O 2 Using Isothermal Microcalorimetry, Ultra-High Precision Coulometry, and Long-Term Cycling," *J. Electrochem. Soc.,* vol. 167, no. 6, 060530, 2020, doi: 10.1149/1945-7111/ab8620.

[33] X. Zhu, Y. Zhong, H. Zhai, Z. Yan, D. Li, "Nanoflake Nickel Hydroxide and Reduced Graphene Oxide Composite as Anode Materials for High Capacity Lithium Ion Batteries," *Electrochim. Acta,* vol. 132, pp. 364–369, 2014, doi: 10.1016/j.electacta.2014.03.132.

[34] M. Y. Cheng, Y. S. Ye, T. M. Chiu, C. J. Pan, B. J. Hwang, "Size Effect of Nickel Oxide for Lithium Ion Battery Anode," *J. Power Sources,* vol. 253, pp. 27–34, 2014, doi: 10.1016/j.jpowsour.2013.12.037.

[35] I. Meer and R. Nazir, "Removal Techniques for Heavy Metals from Fly Ash," *J. Mater. Cycles Waste Manag.,* vol. 20, pp. 703–722, 2018, doi: 10.1007/s10163-017-0651-z.

[36] Y. Han, X. Liu, Z. Lu, "Systematic Investigation of Prelithiated SiO2 Particles for High-Performance Anodes in Lithium-Ion Battery," *Appl. Sci.,* vol. 8, no. 8, 1245, 2018, doi: 10.3390/app8081245.

[37] A. Purwanto, S. S. Nisa, I. P. Lestari, M. N. Ikhsanudin, C. S. Yudha, H. Widiyandari, "High Performance Nickel Based Electrodes in State-of-the-Art Lithium-Ion Batteries: Morphological Perspectives," *KONA Powder Part. J.,* vol. 39, pp. 130-149, 2022, doi: 10.14356/kona.2022015.